

1
2
3
4
5
6
7
8
9
10
11
12
13
14
15
16
17
18
19
20
21
22
23

Supporting Information for

**A New High-Resolution Multi-Meteorological Drought Indices Dataset for
Mainland China**

Contents of this file

Fig. S1–S4

Methods

Standardized precipitation index (SPI)

Standardized precipitation evapotranspiration index (SPEI)

Evaporative demand drought index (EDDI)

Palmer drought severity index (PDSI)

Self-calibrating Palmer drought severity index (SC-PDSI)

Vapor pressure deficit (VPD)

Slope of the saturated vapor pressure

Psychrometric constant

Vapor pressure of the air

Net radiation at the ground surface

Introduction

Here we provide detailed formulas for calculating all the drought indices, with additional figures to support the main content of our paper, “**A New High-Resolution Multi-Meteorological Drought Indices Dataset for Mainland China.**”

24 **Standardized precipitation index (SPI)**

25 The distribution of precipitation is generally not a normal distribution but a skewed
26 distribution. Therefore, in precipitation analysis, drought monitoring, and assessment,
27 the distribution probability Γ is used to describe the change of precipitation. The
28 standardized precipitation index (SPI; McKee et al. 1993) is used to calculate the
29 distribution probability Γ of precipitation within a certain period of time, perform
30 normal standardization, and finally classify the drought level with the standardized
31 precipitation cumulative frequency distribution.

$$32 \quad f(x) = \frac{1}{\beta^\gamma \Gamma(\gamma)} x^{\gamma-1} e^{-x/\beta} \quad x > 0 \quad (1)$$

33 where $\beta > 0$ and $\gamma > 0$ are scale and shape parameters, respectively. β and γ can be
34 obtained by the maximum likelihood estimation method: $\hat{\gamma} = \left[\frac{1}{4A} \left(1 + \sqrt{1 + \frac{4A}{3}} \right) \right]$, $\hat{\beta} =$

$$35 \quad \frac{\bar{x}}{\hat{\gamma}}, \quad A = \lg \bar{x} - \frac{1}{n} \sum_{i=1}^n \lg x_i$$

36 where x_i is a precipitation data sample and \bar{x} is the climate average of precipitation.
37 After the parameters in the probability density function are determined, for the
38 precipitation x_0 in a certain year, the probability of an event in which random variable
39 x less than x_0 can be calculated as follows:

$$40 \quad f(x < x_0) = \int_0^{x_0} f(x) dx \quad (2)$$

41 The event probability when the precipitation is 0 is estimated using the following
42 formula:

$$43 \quad F(x = 0) = m/n \quad (3)$$

44 where m is the number of samples with precipitation of 0, and n is the total number
45 of samples. The Γ distribution probability is normalized by the normal distribution
46 function: that is, the probability values obtained by Equations (2) and (3) are substituted

47 into the normalized normal distribution function:

$$48 \quad F(x < x_0) = \frac{1}{\sqrt{2\pi}} \int_0^{x_0} e^{-\frac{z^2}{2}} \quad (4)$$

$$49 \quad Z = SPI = S \left(t - \frac{c_0 + c_1 t + c_2 t}{1 + d_1 t + d_2 t^2 + d_3 t^3} \right) \quad (5)$$

50 where $t = \sqrt{\ln \frac{1}{F^2}}$, F is the probability of finding (2) or (3); and when $F > 0.5$, $F = 1 -$

51 F , $S = 1$, when $F \leq 0.5$, $S = -1$. The values of the coefficients are as follows:

52 $c_0 = 2.515517$, $c_1 = 0.802853$, $c_2 = 0.010328$, $d_1 = 1.432788$, $d_2 = 0.189269$, and

53 $d_3 = 0.001308$.

54

55 **Standardized precipitation evapotranspiration index (SPEI)**

56 Both SPI and SPEI use a probability density function to fit time series. SPI uses a
57 parametric Gamma distribution to fit cumulative monthly precipitation time series. SPEI
58 is calculated similarly to SPI (Vicente-Serrano et al., 2010), using the cumulative
59 difference between monthly precipitation and potential evapotranspiration (PET) to
60 replace the precipitation variable, and then using a three-parameter log-logistic
61 distribution to fit the data, and then using the inverse cumulative probability density
62 function of the standard normal distribution to convert to the drought index value (Li et
63 al., 2020). First, the PET is calculated. The second step is to calculate the difference
64 between precipitation (P) and PET, $D = P - PET$. The third step is to transform data D
65 as SPI:

$$66 \quad F(x) = \left[1 + \left(\frac{\alpha}{x - \gamma} \right)^\beta \right]^{-1} \quad (6)$$

67 T is the probability of a definite D value:

$$68 \quad T = 1 - F(x) \quad (7)$$

69 For $T \leq 0.5$,

70
$$W = \sqrt{-2 \ln(T)} \quad (8)$$

71

72
$$SPEI = W - \frac{(c_2W + c_1)W + c_0}{[(d_3W + d_2)W + d_1]W + 1} \quad (9)$$

73 For $T > 0.5$,

74
$$W = \sqrt{-2 \ln(1 - T)} \quad (10)$$

75
$$SPEI = - \left(W - \frac{(c_2W + c_1)W + c_0}{[(d_3W + d_2)W + d_1]W + 1} \right) \quad (11)$$

76

77 Values of coefficients are follows: $c_0 = 2.515517$, $c_1 = 0.802853$, $c_2 = 0.010328$,
 78 $d_1 = 1.432788$, $d_2 = 0.189269$, and $d_3 = 0.001308$.

79

80

81 **Evaporative demand drought index (EDDI)**

82 In recent years, the indices for monitoring drought have mainly focused on water
 83 imbalance, because the physical actual evapotranspiration (AET)-based drought signal
 84 indices are used more and more frequently. These include the SPEI, soil water deficit
 85 index, evapotranspiration deficit index, remote sensing global drought severity index,
 86 etc. Although SPEI monitors drought on the basis of the difference between precipitation
 87 (P) and PET, PET is calculated on the basis of some formula or model; for example, PET
 88 obtained by Thornthwaite's method is estimated on the basis of average temperature,
 89 while reference crop evapotranspiration (ET_0) is not directly measured or represented by
 90 a separate index. An index based only on physical ET_0 measurements will have several
 91 advantages: first, the physically based ET_0 index does not need to consider the
 92 availability of surface water, because it focuses on the atmospheric water demand rather
 93 than the difference between surface water supply and demand. Second, it avoids the

94 difficulties inherent in remote sensing data: some remote sensing data are affected by
95 various factors, such as satellite remote sensing data being limited by cloud cover or the
96 time interval when the satellite passes over the ground. This may lead to data delays or
97 missing data. The physically based ET_0 index avoids the difficulties of relying on these
98 data, because it does not need to use remote sensing data to infer water demand. EDDI
99 was developed by Hobbins et al. (2016) as an indicator of atmospheric drying potential,
100 which can indicate plant stress on the ground.

101 The rationale for this indicator is based on two main physical feedbacks between
102 AET and ET_0 : under conditions of water resource constraint (protracted drought), AET
103 and ET_0 change in opposite directions (Bouchet 1963), and under conditions of energy
104 constraint at the onset of a sudden drought, they are in parallel (Fig. S4). Specifically,
105 the magnitude of AET depends on the availability of energy (usually solar radiation, etc.)
106 or water. If water limits evaporation, then atmospheric evaporation demand either plays
107 a role in determining actual evaporation or is a reflection of it. For example, under non-
108 water-constrained conditions, ET_0 estimates the upper limit of (energy-constrained) AET,
109 whereas under water-constrained conditions, land-atmosphere feedbacks from AET lead
110 ET_0 towards opposite or complementary directions. If we use the examples of persistent
111 and sudden droughts, persistent droughts indicate persistent deficits in soil moisture (SM)
112 and fluxes associated with land-air interfaces, where water constraints affect AET.
113 However, “rapid droughts” (i.e., rapidly developing droughts caused by strong, transient
114 meteorological/radiometric changes, such as increasing temperature, wind speed,
115 radiation or moisture decrease, without substantial change in precipitation) tend not to
116 be affected by water constraints. Nevertheless, ET_0 exhibited positive signals in both
117 sustained and rapid droughts, indicating its value in monitoring droughts and as an early
118 indicator of the development of drought conditions (Hobbins et al., 2016).

119

120 **Palmer drought severity index (PDSI)**

121 PDSI is a drought index with clear physical meaning established by Palmer, (1965).

122 It comprehensively considers many factors such as precipitation, soil moisture, runoff,

123 and potential evapotranspiration; it can reflect the impact of pre-season precipitation and

124 water supply and demand on later-period related factors; and it can effectively judge

125 long-term drought conditions (Aiguo et al., 2004).

126 The water balance equation for water supply and demand to reach climate

127 adaptation is as follows:

128
$$P' = \alpha_i PET + \beta_i PR + \gamma_i PRO - \delta_i PL \quad (12)$$

129 P' represents the climate-suitable precipitation, and α_i , β_i , γ_i , and δ_i are the water

130 balance coefficients of each month i ($i = 1, 2, 3, \dots, 12$), which can be defined as follows:

131
$$\alpha_i = \frac{\overline{ET}_i}{\overline{PET}_i}, \beta_i = \frac{\overline{R}_i}{\overline{PR}_i}, \gamma_i = \frac{\overline{RO}_i}{\overline{PRO}_i}, \delta_i = \frac{\overline{L}_i}{\overline{PL}_i} \quad (13)$$

132 ET , RO , R , and L are respectively the actual evapotranspiration, actual flow, actual soil

133 water replenishment, and actual soil water loss in month i . PET , PRO , PR , and PL are

134 respectively the potential evapotranspiration, potential runoff, potential soil water

135 replenishment, and potential soil water loss. In this model, $PR = AWC - (S_s + S_u)$,

136 $PRO = AWC - PR = S_s + S_u$, $PL = PL_s + PL_u$, $PL_s = \min(PE, S_s)$, $PL_u = (PE -$

137 $PL_s)S_u/AWC$, S_s is the initial effective upper soil water content, and S_u is the initial

138 effective lower soil water content. According to the AWC data recommended by Li et

139 al., (2023) we adopted the Global Gridded Surfaces of Selected Soil Characteristics data

140 (https://daac.ornl.gov/cgi-bin/dsviewer.pl?ds_id=1006).

141 Water deficit (d) is the difference between actual precipitation (P) and climate-

142 appropriate precipitation (P'). In order to make PDSI a standardized index, after finding

143 the water deficit, we multiply it by the climate weight coefficient K of a given month in

144 a given place, and thus obtain the water anomaly index Z , also known as Palmer Z index,
 145 which indicates the deviation degree between the actual climate dry–wet condition and
 146 its average water condition in a given month and place: $Z = dK$; the value of K is
 147 determined by the month and geographical location:

$$148 \quad K_i = \frac{a}{\sum_{j=1}^{12} \bar{D}_j K'_j} K'_i \quad (14)$$

149 The empirical constant $a = 17.67$ obtained by Palmer from the data of nine stations
 150 in seven states was revised to 16.84 according to the climate characteristics of China
 151 (Zhong et al., 2019), where $\sum_{j=1}^{12} \bar{D}_j K'_j$ is the average annual absolute moisture anomaly
 152 over the years, with j representing January to December;

$$153 \quad K'_i = 1.6 \log_{10} \left(\frac{\overline{PET}_i + \bar{R}_i + \overline{RO}_i}{\bar{P}_i + \bar{L}_i} + 2.8 \right) + 0.4 \quad (15)$$

154 where \bar{D}_i the multi-year average of the absolute value of the moisture anomaly d in
 155 month i . Finally, the PDSI value for each month is calculated as follows:

$$156 \quad X_i = pX_{i-1} + qZ_i \quad (16)$$

157 p and q are the duration factors that affect PDSI sensitivity. Palmer obtained p as 0.897
 158 and q as 1/3 based on two stations in central Iowa and western Kansas, but we revised
 159 them to $p = 0.755$ and $q = 1/1.63$ on the basis of data from weather stations in China.

160 PDSI is a cumulative index: that is, an index where each successive value is based on
 161 the previous value. Specifically, any given PDSI value (X_i) is the weighted sum of the
 162 previous PDSI value (X_{i-1}) and the current humidity anomaly Z_i . For example, the
 163 current PDSI value (X_i) is equal to q times the current water vapor outlier Z_i plus p
 164 times the previous PDSI value (X_{i-1}).

165

166 **Self-calibrating palmer drought severity index (SC-PDSI)**

167 Based on PDSI, Wells et al. (2004) proposed and evaluated an SC-PDSI. Wells et al.
 168 (2004) believed that changing the ratio (\tilde{K}) could solve the spatial inconsistency of PDSI
 169 without changing the way PDSI deals with seasonal climate changes.

$$170 \quad \tilde{K} = \frac{a}{\sum_{j=1}^{12} \bar{d}_j K'_j} K'_i \quad (17)$$

171 Since $\sum_{j=1}^{12} \bar{d}_j K'_j$ can be approximately regarded as the annual sum of the average
 172 absolute value of Z ($\tilde{Z} = \sum_{j=1}^{12} \bar{d}_j K'_j$), and the value of a , 17.67 as obtained by Palmer,
 173 is the average value of \tilde{Z} (i.e., the annual average sum of vapor anomalies), and since
 174 PDSI is based on cumulative vapor anomalies, so $\tilde{K} = \frac{\text{expected average PDSI}}{\text{observed average PDSI}}$. If the non-
 175 extreme value range of PDSI is defined as -4 to 4 , but in practice this range is different.
 176 Palmer (1965) argues that if the PDSI were truly a standardized measure of drought
 177 severity, then values outside of that range (-4 to 4) would occur with roughly the same
 178 frequency. If the frequency of extreme events is f_e , then the f_e th percentile should be
 179 -4.00 and the $(100 - f_e)$ th percentile should be 4.00 . So $\tilde{K} =$
 180 $\frac{\text{expected } f_e \text{th percentile of the PDSI}}{\text{observed } f_e \text{th percentile of the PDSI}}$. Defining an extreme drought as a "one in 50 year
 181 event" does not determine the percentage of PDSI values below -4.00 , as it may last two
 182 months or two years. In this implementation, Wells et al. (2004) used an f_e value of 2%,
 183 which resulted in the following climate characterization equation:

$$184 \quad K = \begin{cases} K'(-4 / 2nd \text{ percentile}), & \text{if } d < 0 \\ K'(4 / 98th \text{ percentile}), & \text{if } d \geq 0 \end{cases} \quad (18)$$

185 Palmer found the duration factor empirically, based on the linear relationship between
 186 the length of time and severity of the most extreme droughts he studied in Kansas and
 187 Iowa. To estimate the severity of droughts, he summarized the Z -scores for severe
 188 droughts and derived the following linear relationship:

189
$$PDSI = -4.0 \Rightarrow \sum_{i=1}^t Z_i = -1.236t - 10.764 \quad (19)$$

190
$$PDSI = -3.0 \Rightarrow \sum_{i=1}^t Z_i = -0.927t - 8.073 \quad (20)$$

191
$$PDSI = -2.0 \Rightarrow \sum_{i=1}^t Z_i = -0.618t - 5.382 \quad (21)$$

192
$$PDSI = -1.0 \Rightarrow \sum_{i=1}^t Z_i = -0.309t - 2.691 \quad (22)$$

193
$$\sum_{i=1}^t Z_i = (0.309t + 2.691)X_t \quad (23)$$

194 The linear relationship from (19) to (23) can be simplified to (24), respectively, for a
 195 given PDSI value $X_t = -4, -3, -2,$ and -1 .

196
$$\sum_{i=1}^t Z_i = (mt + b) \frac{X_t}{C} \quad (24)$$

197 It is not difficult to find that when $C = -4, m = -1.236,$ and $b = -10.764,$ (24) is equal
 198 to (19); (24) can also be derived in a generalized form as follows:

199
$$X_t = \left(1 - \frac{m}{m+b}\right)X_{t-1} + \frac{C}{m+b}Z_t \quad (25)$$

200 Thus, the persistence factor $p = \left(1 - \frac{m}{m+b}\right), q = \frac{C}{m+b}$.

201 In practical analysis, because different regions have different sensitivities to
 202 precipitation events, and some regions have different sensitivities to precipitation and
 203 non-precipitation periods, two sets of duration factors are needed. SC-PDSI establishes
 204 a separate duration factor for dry and wet periods, so that the sensitivity of the index
 205 depends on local climate and has different sensitivities to wetness and moisture deficit.

206 We summarize the calculation steps of SC-PDSI as follows, after Wells et al. (2004):

207 (1) First, calculate moisture departures according to (12) and (13), $d = P - P'$;

- 208 (2) Calculate K according to K' in (15), and then calculate the moisture anomaly index,
 209 $Z = dK$;
- 210 (3) Calculate the index duration factor using the least squares method under extremely
 211 wet and extremely dry conditions: $\sum_{i=1}^t Z_i = mt + b$, which will give two sets of
 212 parameters m and b . Calculate m and b according to the results of (13);
- 213 (4) Substitute m and b into Equation (25) to calculate PDSI;
- 214 (5) Recalculate K according to (18) after finding the 98th and 2nd percentiles of PDSI;
- 215 (6) Substitute the results of (10) into $Z = dK$ to get the new Z ;
- 216 (7) Return to step 3 again to get the new m and b , and finally get SC-PDSI.

217

218 **Vapor pressure deficit (VPD)**

219 Saturated vapor pressure is a function of temperature and can be directly calculated
 220 from temperature, as shown in the Tetens empirical formula (Allen et al., 1998):

$$221 \quad e^0(T) = 0.6108 \exp\left[\frac{17.27T}{T + 237.3}\right] \quad (26)$$

222 where T is the air temperature ($^{\circ}\text{C}$), and $e^0(T)$ is the saturated water vapor pressure
 223 at temperature (kPa). Since the above equation is a nonlinear function, for the average
 224 saturated vapor pressure with such a long interval at the monthly scale, if the average
 225 temperature is used to replace the daily maximum and minimum temperatures, the
 226 estimated value of the average saturated vapor pressure will be low, and the
 227 corresponding vapor pressure difference will be small. Therefore, the mean value of the
 228 saturated vapor pressure corresponding to the daily average maximum and minimum
 229 temperatures within the time interval is used for calculation (Li et al., 2014):

$$230 \quad e_s = \frac{e^0(T_{max}) + e^0(T_{min})}{2} \quad (27)$$

231 where, e_s is the average saturated vapor pressure (kPa), and T_{max} and T_{min} are the

232 daily average highest and lowest air temperature ($^{\circ}\text{C}$), respectively. The actual vapor
 233 pressure e_a (kPa) is calculated according to the monthly average relative humidity
 234 (φ_{mean}): $e_a = e_s \frac{\varphi_{mean}}{100}$, and $\text{VPD} = e_s - e_a$.

235

236 Slope of the saturated vapor pressure

$$\Delta = \frac{4098 \times [0.6108 \times \exp(\frac{17.27T}{T + 237.3})]}{(T + 237.3)^2} \quad (28)$$

237 where Δ is the slope of the saturated vapor pressure temperature relationship (kPa ·
 238 $^{\circ}\text{C}^{-1}$)

239

240 Psychrometric constant

$$\gamma = \frac{c_p P}{\varepsilon \lambda} = 0.665 \times 10^{-3} P \quad (29)$$

$$P = 101.3 \times \left(\frac{293 - 0.0065z}{293}\right)^{5.26} \quad (30)$$

241 where γ is the psychrometric constant (kPa · $^{\circ}\text{C}^{-1}$); λ is the latent heat of evaporation
 242 ($2.45 \text{ MJ} \cdot \text{kg}^{-1}$); ε is the molecular weight ratio of water to air (0.622); c_p is the
 243 specific heat of air at constant pressure ($1.013 \times 10^{-3} \text{ MJ} \cdot \text{kg}^{-1} \cdot ^{\circ}\text{C}^{-1}$); P is atmospheric
 244 pressure (kPa); and z is local elevation (m).

245

246 Vapor pressure of the air

$$e^o(T) = 0.618 \exp\left(\frac{17.27T}{T + 237.3}\right) \quad (31)$$

$$e_a = \frac{RH_{mean}}{100} [e^o(T)] \quad (32)$$

$$e_s = \frac{e^o(T_{max}) + e^o(T_{min})}{2} \quad (33)$$

247 where RH_{mean} is the mean daily relative humidity; T_{max} is the maximum temperature
 248 ($^{\circ}\text{C}$); T_{min} is the minimum temperature ($^{\circ}\text{C}$); and $e^o(T)$ is the saturation vapor
 249 pressure function (kPa).

250

251 **Net radiation at the ground surface**

252 The first step is to calculate the extraterrestrial radiation (R_a). The daily
 253 extraterrestrial radiation at different latitudes during the year can be estimated from the
 254 solar constant, the magnetic declination of the sun, and the day's position during the year.

$$R_a = \frac{24 \times 60}{\pi} G_{sc} d_r [\omega_s \sin(\varphi) \sin(\delta) + \cos(\varphi) \cos(\delta) \sin(\omega_s)] \quad (34)$$

255 where R_a is extraterrestrial radiation ($\text{MJ} \cdot \text{m}^{-2} \text{day}^{-1}$); G_{sc} is the solar constant and
 256 takes the value of $0.082 \text{ (MJ} \cdot \text{m}^{-2} \text{min}^{-1}\text{)}$; d_r is the average distance between the Earth
 257 and the sun, calculated by equation (35); δ is the magnetic declination of the sun (rad),
 258 calculated by formula (36); φ is latitude (rad); and ω_s is the sunset hour angle,
 259 calculated by formula (37).

$$d_r = 1 + 0.033 \cos\left(\frac{2\pi}{365} J\right) \quad (35)$$

$$\delta = 0.408 \sin\left(\frac{2\pi}{365} J - 1.39\right) \quad (36)$$

260 where J indicates the day order, ranging from 1 to 365 or 366.

$$\omega_s = \arccos[-\tan(\varphi)\tan(\delta)] \quad (37)$$

261 If the observed value of solar radiation R_s is not available, it can be obtained from
 262 the formula for the relationship between solar radiation and extraterrestrial radiation and
 263 relative insolation:

$$R_s = \left(a_s + b_s \frac{n}{N}\right) R_a \quad (38)$$

264 where n is actual sunshine hours (h); N is the maximum possible sunshine hours; and a_s

265 and b_s vary with atmospheric conditions (humidity, dust) and the sun's magnetic
 266 declination (latitude and month). When there are no actual solar radiation data and
 267 empirical parameters to use, it is recommended to use $a_s = 0.25$ and $b_s = 0.5$.

268 Net short-wave radiation at the surface is calculated by the balance of received and
 269 reflected solar radiation:

$$R_{ns} = (1 - \alpha)R_s \quad (39)$$

270 where R_{ns} is net solar radiation or shortwave radiation ($\text{MJ} \cdot \text{m}^{-2} \text{day}^{-1}$); and α is
 271 albedo, where the albedo of the reference crop of green grassland is 0.23.

272 When near sea level or when empirical parameters are available for a_s and b_s , the
 273 clear-sky solar radiation is calculated by the following formula:

$$R_{so} = (a_s + b_s)R_a \quad (40)$$

274 where R_{so} is clear-sky solar radiation ($\text{MJ} \cdot \text{m}^{-2} \text{day}^{-1}$).

275 The net long-wave radiation (R_{nl}) is calculated as follows. Long-wave radiation is
 276 proportional to the 4th power of the absolute surface temperature, and this relationship
 277 can be quantified by the Stefan-Boltzmann law. However, due to atmospheric absorption
 278 and downward radiation, the net energy flux at the surface is less than the value
 279 calculated using the Stefan-Boltzmann law. Water vapor, clouds, carbon dioxide, and
 280 dust all absorb and emit long-wave radiation, and their concentrations should be known
 281 when estimating net expended radiation fluxes. Due to the large influence of humidity
 282 and cloud cover, these two factors are used to estimate the net expenditure flux of long-
 283 wave radiation using the Stefan-Boltzmann law, and the concentration of other absorbers
 284 is assumed to be constant:

$$R_{nl} = \sigma \left[\frac{T_{max,K}^4 + T_{min,K}^4}{2} \right] (0.34 - 0.14\sqrt{e_a}) \left(1.35 \frac{R_s}{R_{so}} - 0.35 \right) \quad (41)$$

285 where σ is the Stefan-Boltzmann constant with a value of 4.903×10^{-9} ($\text{MJ} \cdot$

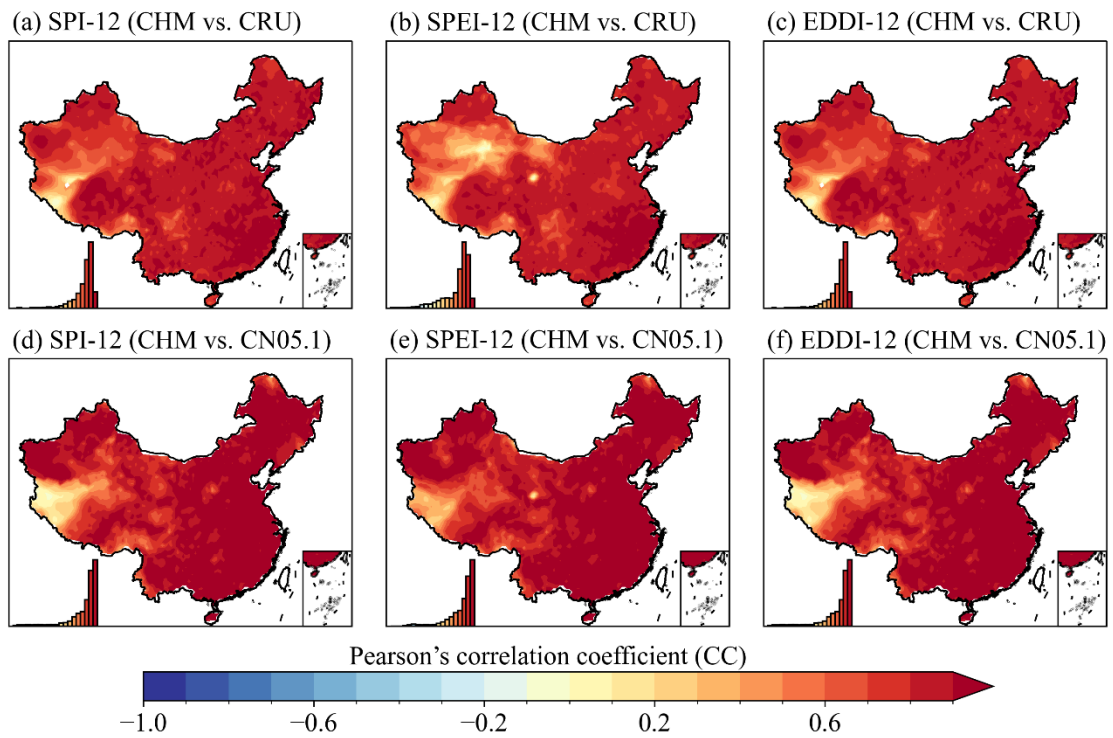
286 $K^{-4}m^{-2}day^{-1}$); $T_{max,K}$ is the highest absolute temperature in a day (24 hours) in
287 Kelvin (K) ($K = ^\circ C + 273.16$); $T_{min,K}$ is the lowest absolute temperature in a day (24
288 hours) in Kelvin (K) ($K = ^\circ C + 273.16$); and $(0.34 - 0.14\sqrt{e_a})$ is the corrected term for
289 air humidity: if the air humidity increases, the value of this term will become smaller;
290 $(1.35 \frac{R_s}{R_{s0}} - 0.35)$ is the revised term for the cloud cover, and if the amount of cloud
291 increases, R_s will decrease and the value of this term will decrease accordingly.

292 The net radiation R_n is the difference between the incoming short-wave net
293 radiation R_{ns} and the outgoing long-wave net radiation R_{nl} :

$$R_n = R_{ns} - R_{nl} \quad (42)$$

294

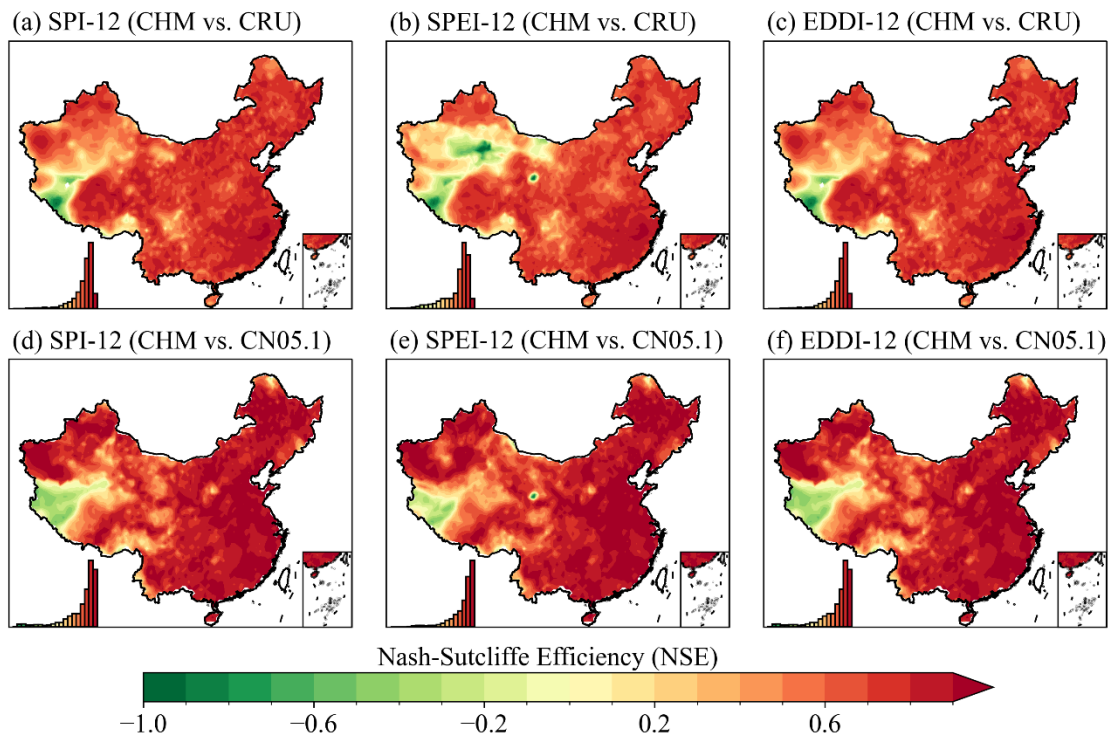
295



296

297 **Fig. S1.** (a–c) Correlation spatial distributions of SPI-12, SPEI-12, and EDDI-12 based
 298 on CHM and CRU data. (d–f) Correlation spatial distributions of SPI-12, SPEI-12, and
 299 EDDI-12 based on CHM and CN05.1 data.

300



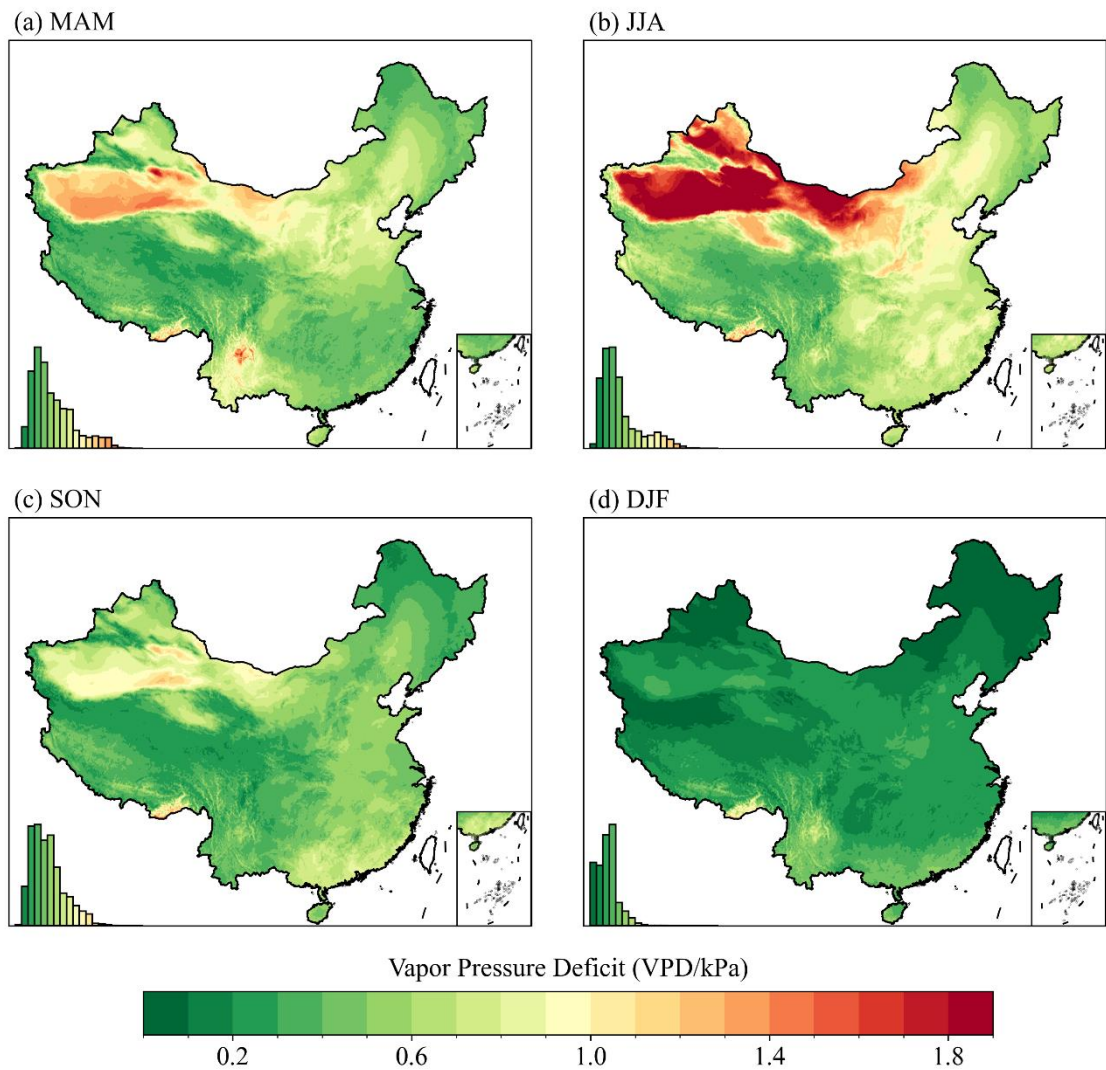
301

302 **Fig. S2.** (a–c) Spatial distributions of NSE of SPI-12, SPEI-12, and EDDI-12 based on

303 CHM and CRU data. (d–f) Spatial distributions of NSE of SPI-12, SPEI-12, and EDDI-

304 12 based on CHM and CN05.1 data.

305



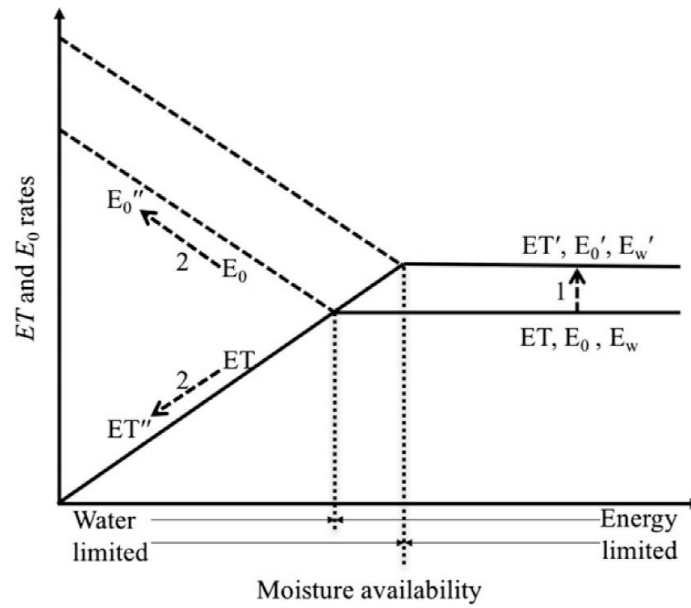
306

307 **Fig. S3.** Spatial distribution of seasonal VPD in China, 1961–2022. (a) Spring (March–

308 April–May, MAM). (b) Summer (June–July–August, JJA). (c) Autumn (September–

309 October–November, SON). (d) Winter (December–January–February, DJF).

310



311

312 **Fig. S4.** Idealized parallel and complementary responses of AET and ET_0 (E_0 in figure)
 313 to varying moisture and energy conditions. Figure adapted from Hobbins et al. (2016).

314 **References**

- 315 Aiguo, D., Kevin, E. T., and Taotao, Q.: A Global Dataset of Palmer Drought Severity
316 Index for 1870 – 2002 : Relationship with Soil Moisture and Effects of Surface
317 Warming, *J Hydrometeorol*, 5, 1117–1130,
318 <https://doi.org/10.1016/j.molcel.2017.04.015>, 2004.
- 319 Dai, A.: Drought under global warming: A review, <https://doi.org/10.1002/wcc.81>, 2011.
- 320 Hobbins, M. T., Wood, A., McEvoy, D. J., Huntington, J. L., Morton, C., Anderson, M.,
321 and Hain, C.: The evaporative demand drought index. Part I: Linking drought
322 evolution to variations in evaporative demand, *J Hydrometeorol*, 17, 1745–1761,
323 <https://doi.org/10.1175/JHM-D-15-0121.1>, 2016.
- 324 Li, L., She, D., Zheng, H., Lin, P., and Yang, Z.-L.: Elucidating Diverse Drought
325 Characteristics from Two Meteorological Drought Indices (SPI and SPEI) in China,
326 *J Hydrometeorol*, 21, 1513–1530, <https://doi.org/10.1175/jhm-d-19-0290.1>, 2020.
- 327 Mckee, T., Doesken, N., Kleist, J., 1993. The relationship of drought frequency and
328 duration to time scales Proceedings of the 8th Conference on Applied Climatology.
329 American Meteorological Society, Boston, MA.
- 330 Palmer, W.C., 1965. Meteorological Drought. US Department of Commerce, Weather
331 Bureau, Washington, DC.
- 332 Vicente-Serrano, S. M., Beguería, S., and López-Moreno, J. I.: A multiscalar drought
333 index sensitive to global warming: The standardized precipitation
334 evapotranspiration index, *J Clim*, 23, 1696–1718,
335 <https://doi.org/10.1175/2009JCLI2909.1>, 2010.
- 336 Wells, N., Goddard, S., and Hayes, M. J.: A self-calibrating Palmer Drought Severity
337 Index, *J Clim*, 17, 2335–2351, [https://doi.org/10.1175/1520-0442\(2004\)017<2335:ASPDSI>2.0.CO;2](https://doi.org/10.1175/1520-0442(2004)017<2335:ASPDSI>2.0.CO;2), 2004.

339 Zhong, R., Chen, X., Lai, C., Wang, Z., Lian, Y., Yu, H., and Wu, X.: Drought monitoring
340 utility of satellite-based precipitation products across mainland China, J Hydrol,
341 568, <https://doi.org/10.1016/j.jhydrol.2018.10.072>, 2019.

342